iScience, Volume *24*

Supplemental Information

Rapid subcellular calcium responses and dynamics by calcium sensor G-CatchER^{+}

Florence N. Reddish, Cassandra L. Miller, Xiaonan Deng, Bin Dong, Atit A. Patel, Mohammad A. Ghane, Barbara Mosca, Cheyenne McBean, Shengnan Wu, Kyril M. Solntsev, You Zhuo, Giovanni Gadda, Ning Fang, Daniel N. Cox, Angela M. Mabb, Susan Treves, Francesco Zorzato, and Jenny J. Yang

Supplemental figures and Tables

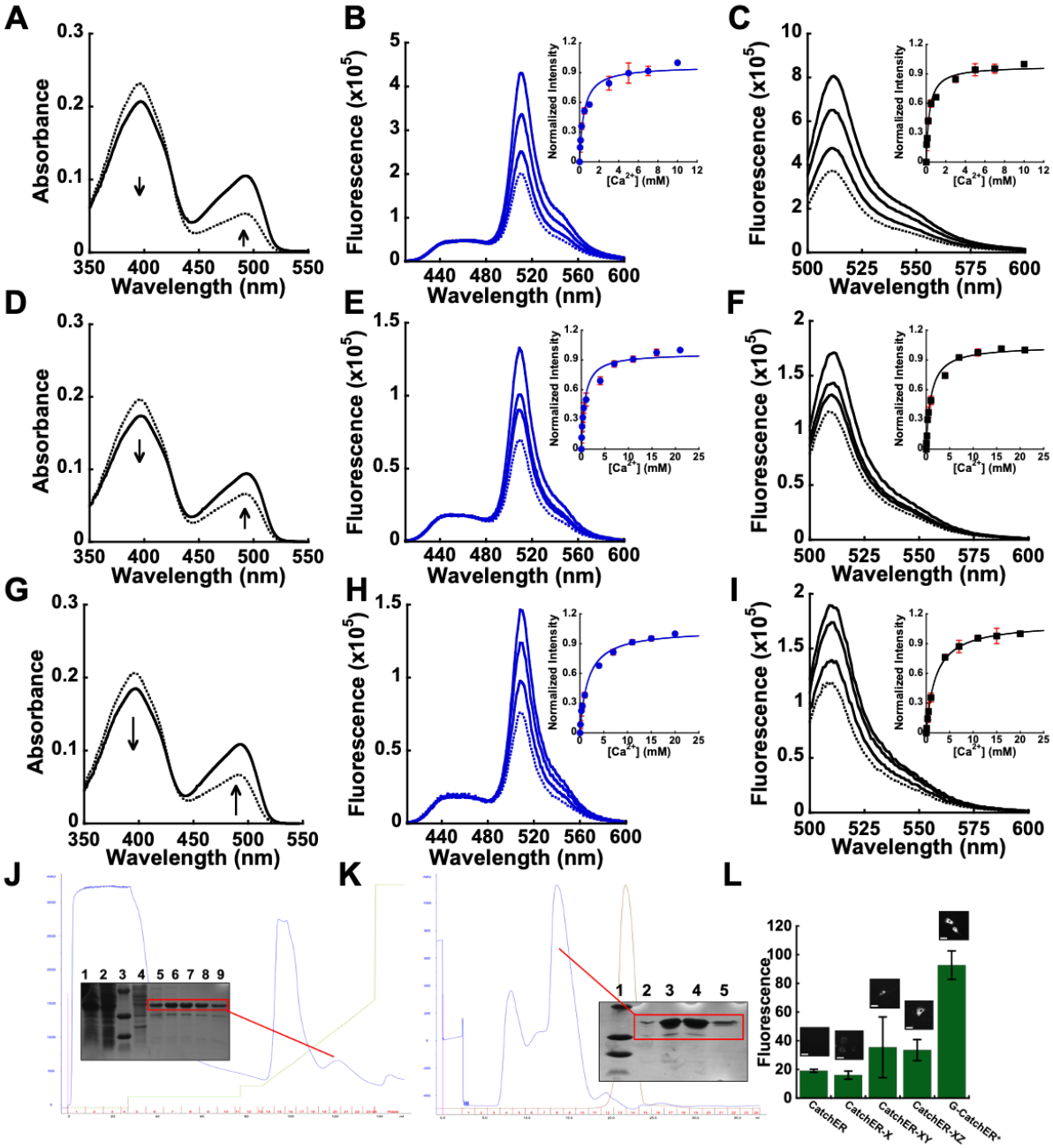

Supplemental Figure 1. In vitro Ca^{2+} K_d and purification of bacterially expressed of CatchER-X (S175G mutation), CatchER-XY (S175G and Y39N mutation) and G-CatchER-XZ (S175G and S30R mutation) variants using fluorescence spectroscopy, related to Figure 1.

Inset, Binding curves were fit with a 1:1 binding equation to obtain the K_d. **A, D, G.** Absorbance spectra of the protein samples before Ca^{2+} titration (dashed line) and after with a saturating amount of Ca^{2+} (solid line). **B** and **C**. Fluorescence increase of S175G in response to 0-7 mM Ca^{2+}. **E** and **F**. Fluorescence increase of S175G S30R in response to 0-10 mM Ca^{2+}. **H** and **I**. Fluorescence increase of S175G Y39N in response to 0-21 mM Ca^{2+}. **J.** HisTag purification of G-CatchER$^+$. Inset SDS-PAGE gel shows samples from different stages of purification. **K.** Size exclusion chromatography of G-CatchER$^+$ using a Superdex 200 column. Inset SDS-PAGE gel shows pure fractions of G-CatchER$^+$ peak in red box corresponding to the chromatogram peak. **L.** Fluorescence intensity plot at 37°C for CatchER, CatchER-X (S175G mutation), CatchER-XY (S175G and Y39N mutation), G-CatchER-XZ (S175G and S30R mutation), and G-CatchER$^+$ (S175G, Y39N and S30R mutations) in C2C12 cells. Scale bars, 20 µm.

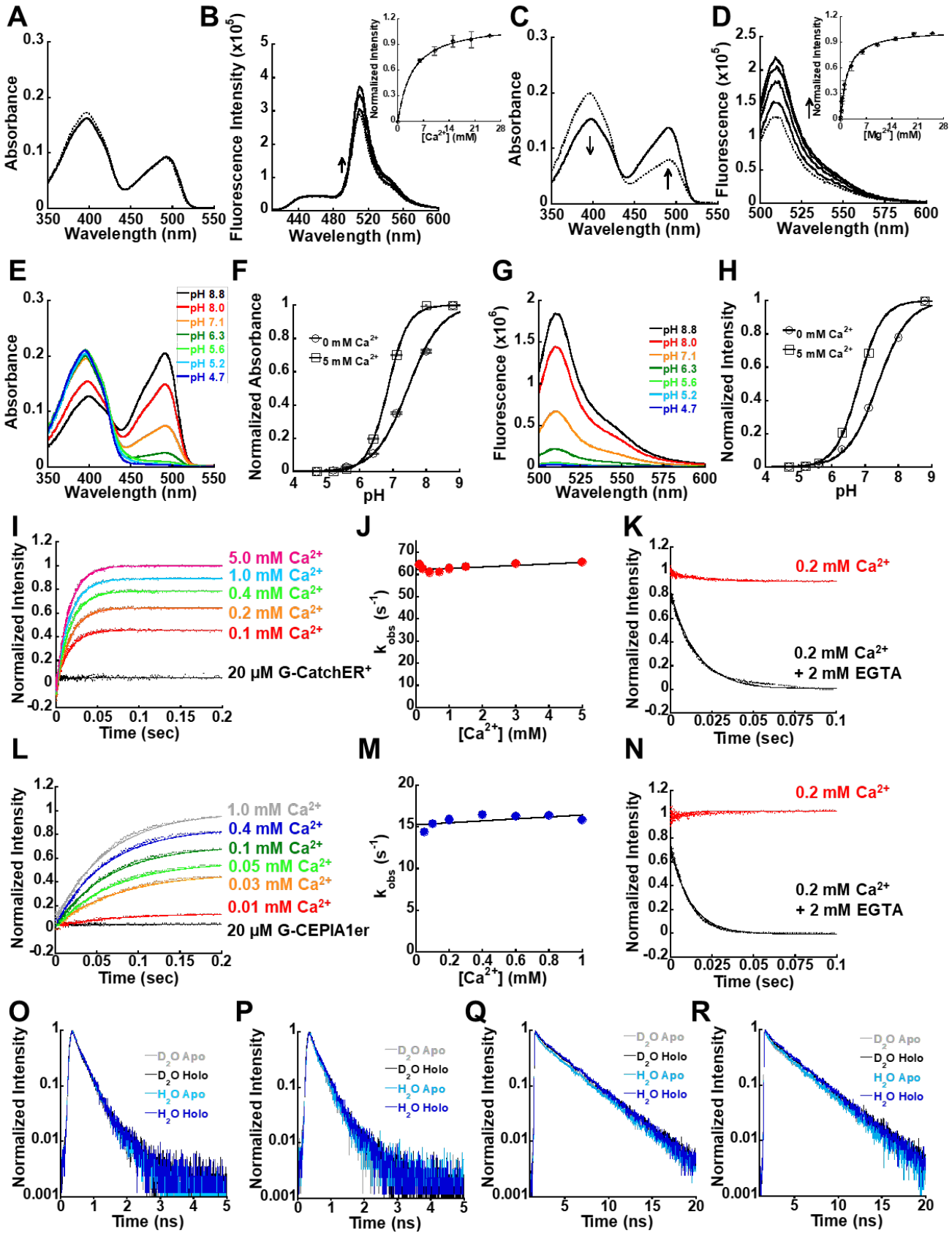
A
Absorbance
Wavelength (nm)
B
Fluorescence Intensity (x10^5)
Wavelength (nm)
Normalized Intensity
[Ca2+] (mM)
C
Absorbance
Wavelength (nm)
D
Fluorescence (x10^5)
Wavelength (nm)
Normalized Intensity
[Mg2+] (mM)
E
pH 8.8
pH 8.0
pH 7.1
pH 6.3
pH 5.6
pH 5.2
pH 4.7
Absorbance
Wavelength (nm)
F
Normalized Absorbance
0 mM Ca2+
5 mM Ca2+
pH
G
Fluorescence (x10^6)
pH 8.8
pH 8.0
pH 7.1
pH 6.3
pH 5.6
pH 5.2
pH 4.7
Wavelength (nm)
H
Normalized Intensity
0 mM Ca2+
5 mM Ca2+
pH
I
Normalized Intensity
5.0 mM Ca2+
1.0 mM Ca2+
0.4 mM Ca2+
0.2 mM Ca2+
0.1 mM Ca2+
20 μM G-CatchER+
Time (sec)
J
kobs (s-1)
[Ca2+] (mM)
K
Normalized Intensity
0.2 mM Ca2+
0.2 mM Ca2+
+ 2 mM EGTA
Time (sec)
L
Normalized Intensity
1.0 mM Ca2+
0.4 mM Ca2+
0.1 mM Ca2+
0.05 mM Ca2+
0.03 mM Ca2+
0.01 mM Ca2+
20 μM G-CEPIA1er
Time (sec)
M
kobs (s-1)
[Ca2+] (mM)
N
Normalized Intensity
0.2 mM Ca2+
0.2 mM Ca2+
+ 2 mM EGTA
Time (sec)
O
Normalized Intensity
D2O Apo
D2O Holo
H2O Apo
H2O Holo
Time (ns)
P
Normalized Intensity
D2O Apo
D2O Holo
H2O Apo
H2O Holo
Time (ns)
Q
Normalized Intensity
D2O Apo
D2O Holo
H2O Apo
H2O Holo
Time (ns)
R
Normalized Intensity
D2O Apo
D2O Holo
H2O Apo
H2O Holo
Time (ns)

Supplemental Figure 2. Optical properties and fluorescence lifetime of G-CatchER$^+$, and Ca^{2+} binding kinetics of G-CatchER$^+$ and G-CEPIA1er, related to Figure 1.

A. Absorbance spectra of 10 μM G-CatchER$^+$ in 10 mM Tris pH 7.4 with 150 mM KCl before (dashed line) and after titrating up to 25 mM Ca^{2+} (solid line). **B.** Fluorescence increase of G-CatchER$^+$ in response to the stepwise addition of up to 25 mM Ca^{2+} in high salt buffer excited at 395 nm monitored at 510 nm emission. *Inset.* Fitting of the normalized fluorescence intensity. The Ca^{2+} K_d in the presence of 150 mM KCl was 3.74 ± 0.70 mM. **C.** Absorbance spectra of 10 μM G-CatchER$^+$ sample in 10 mM Tris pH 7.4 before (dashed line) and after (solid line) titrating up to 25 mM Mg^{2+}. **D.** Fluorescence increase of G-CatchER$^+$ in response to the stepwise addition of up to 25 mM Mg^{2+} in 10 mM Tris pH 7.4 excited at 488 nm monitored at 510 nm emission. *Inset.* Fitting of the normalized fluorescence intensity. Mg^{2+} K_d was 1.78 ± 0.44 mM. **E-H**. The chromophore pK_a of G-CatchER$^+$ was measured by absorbance and fluorescence spectroscopy in the absence and presence of 5 mM Ca^{2+}. **E.** Representative absorbance spectra of G-CatchER$^+$ in the absence of Ca^{2+}. **F.** Normalized 488 nm absorbance data in the absence (●) and presence (■) of 5 mM Ca^{2+}. The calculated pK_a was 7.4 ± 0.0 without Ca^{2+} and 6.8 ± 0.0 with 5 mM Ca^{2+}. **G.** Representative fluorescence spectra of G-CatchER$^+$ in the absence of Ca^{2+} using 488 nm excitation with emission at 510 nm. **H.** Normalized fluorescence intensity data in the absence (●) and presence (■) of 5 mM Ca^{2+}. Calculated pK_a was 7.4 ± 0.0 without Ca^{2+} and 6.8 ± 0.0 with 5 mM Ca^{2+}. **I.** Normalized fluorescence intensity of Ca^{2+} associated kinetics of G-CatchER$^+$ in the presence of different concentrations of Ca^{2+}. **J.** k_{obs} under different concentrations of Ca^{2+}, fitted by a linear curve. **K.** Normalized fluorescence intensity of Ca^{2+} disassociation kinetics of G-CatchER$^+$ in the presence of 2 mM EGTA. **L.** Normalized fluorescence intensity of Ca^{2+} association kinetics of G-CEPIA1er in the presence of different concentrations of Ca^{2+}. **M.** k_{obs} under different concentrations of Ca^{2+}, fitted by a linear curve. **N.** Normalized fluorescence intensity of Ca^{2+} dissociation kinetics of G-CatchER$^+$ in the presence of 2 mM EGTA. **O&P.** G-CatchER **(O)** and G-CatchER$^+$ **(P)** were excited at 372 nm and emitted at 440 nm in the time range of 5 ns. **Q&R.** G-CatchER (**Q**) and G-CatchER$^+$(**R**) were excited at 372 nm and emitted at 510 nm in the time range of 20 ns.

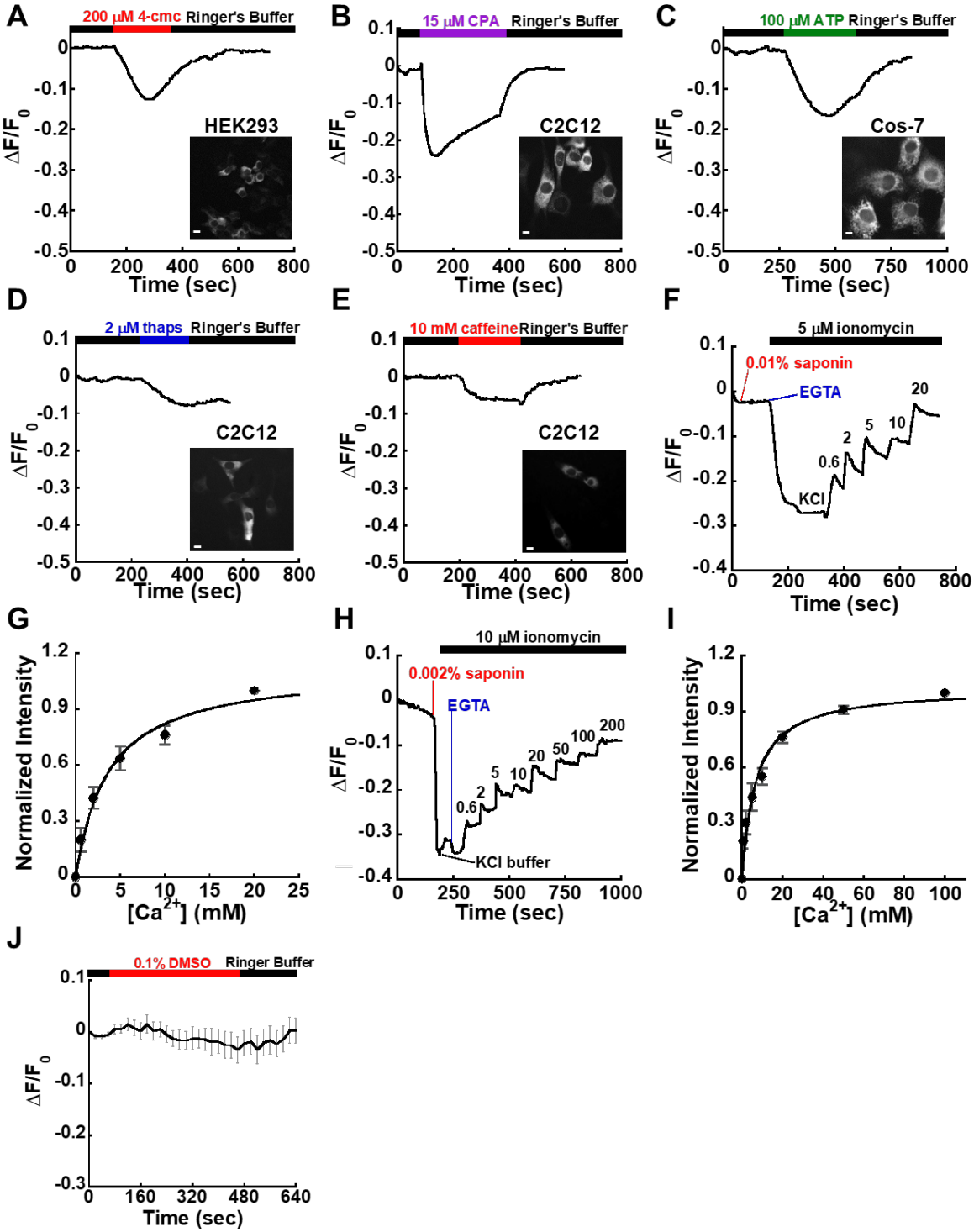

Supplemental Figure 3. *In Situ* validation of G-CatchER$^+$ in response to receptor agonists and antagonists in several cell lines, related to Table 1 and Figure 2.

Representative data plots from cell studies of G-CatchER$^+$ responses to changes in ER Ca^{2+}. **A.** RyR mediated Ca^{2+} release from the ER in HEK293 cells using 4-cmc. **B.** Reversible inhibition of SERCA pump in C2C12 cells using 15 μM of CPA. ER Ca^{2+} is temporarily reduced by blocking SERCA pump function. **C.** 100 μM of ATP was added to initiate a release of Ca^{2+} from the ER in Cos-7 cells. ATP acts on the IP_3R, which indirectly releases Ca^{2+} from the ER after production of IP_3 from P2YR activation. **D.** Irreversible SERCA pump inhibition with 2 μM

thapsigargin in C2C12 cells. After addition of thapsigargin and washing with Ringer's buffer, no ER refilling occurs. E. RyR1 activation with 10 mM caffeine in C2C12 cells. **F-I**. Measurement of the *in situ* K_d of G-CatchER$^+$ in Cos7 (**F** and **G**) and HEK293 cells (**H** and **I**). **F.** 0, 0.6, 2, 6, 10, and 20 mM Ca^{2+} was added to permeabilized Cos7 cells in the presence of 5 µM ionomycin. n = 11. **G.** Intensity from **F** was normalized and fitted with the 1:1 binding equation to get an *in situ* Ca^{2+} K_d of 3.84 ± 1.48 mM. **H.** 0.6, 2, 5, 10, 20, 50, 100, and 200 mM Ca^{2+} was added to permeabilized HEK293 cells in the presence of 10 µM ionomycin. n = 11. **I.** Intensity from **H** was normalized and fitted with the 1:1 binding equation to get an *in situ* Ca^{2+} K_d of 3.23 ± 1.38 mM. **J**. 0.1% DMSO control experiments in C2C12 cells. Scale bars, 20 µm.

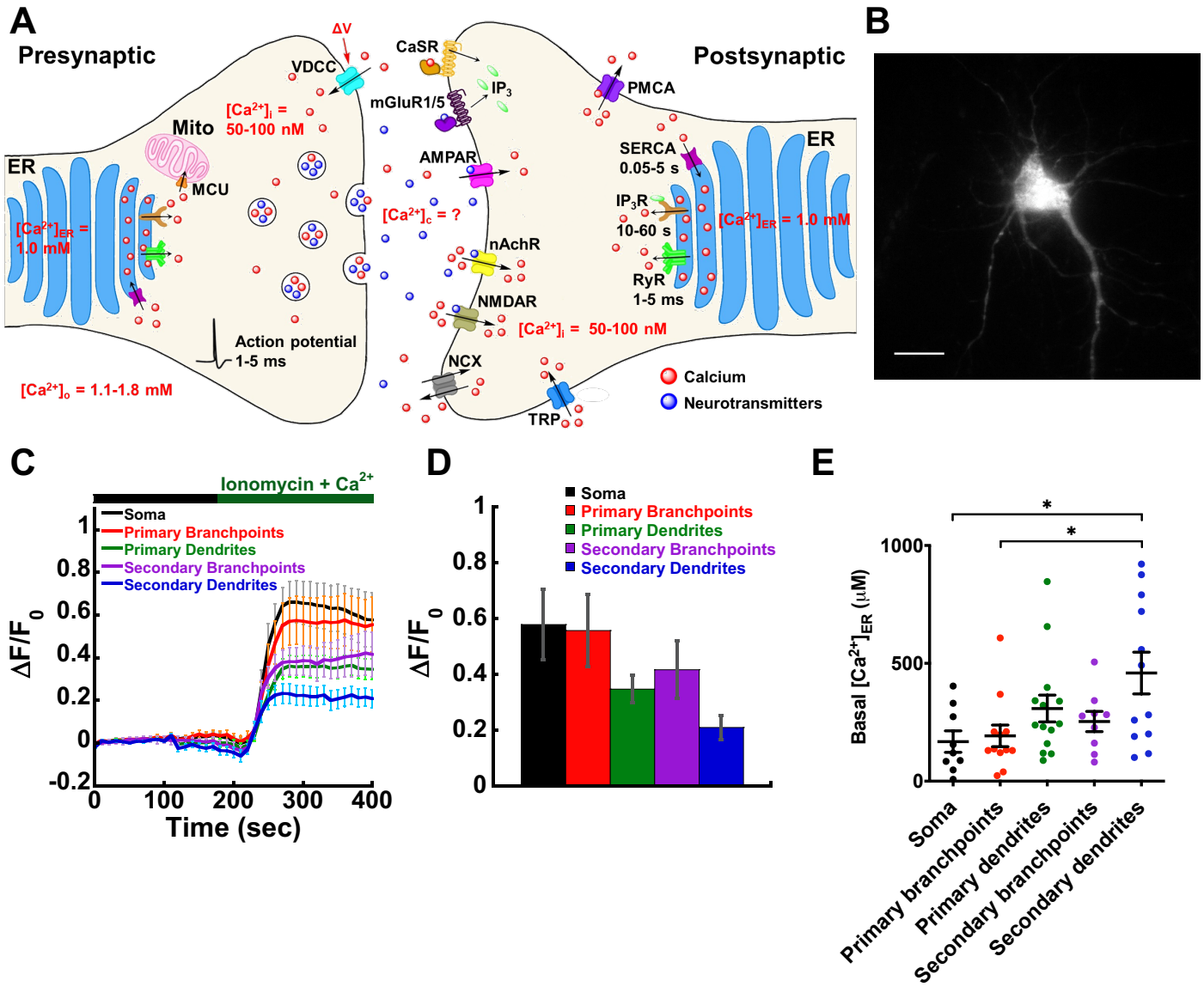

Supplemental Figure 4. Neuron Ca^{2+} signaling and G-CatchER$^+$ response in mouse hippocampal neurons, related to Figure 3.

A. Schematic of Ca^{2+} sources and estimated concentrations at a typical excitatory chemical synapse. **B**. Example of a primary hippocampal neuron cultured 13 days *in vitro* transfected with G-CatchER$^+$. **C&D**. Traces and amplitude of G-CatchER$^+$ in response to 50 μM ionomycin and 10 mM Ca^{2+} in hippocampal neurons. **E.** Estimated absolute ER Ca^{2+} concentration in different neuronal regions using G-CatchER$^+$. Scale bar is 20 μm. Error bars are ± SEM, One-way ANOVA, Tukey's multiple comparisons.

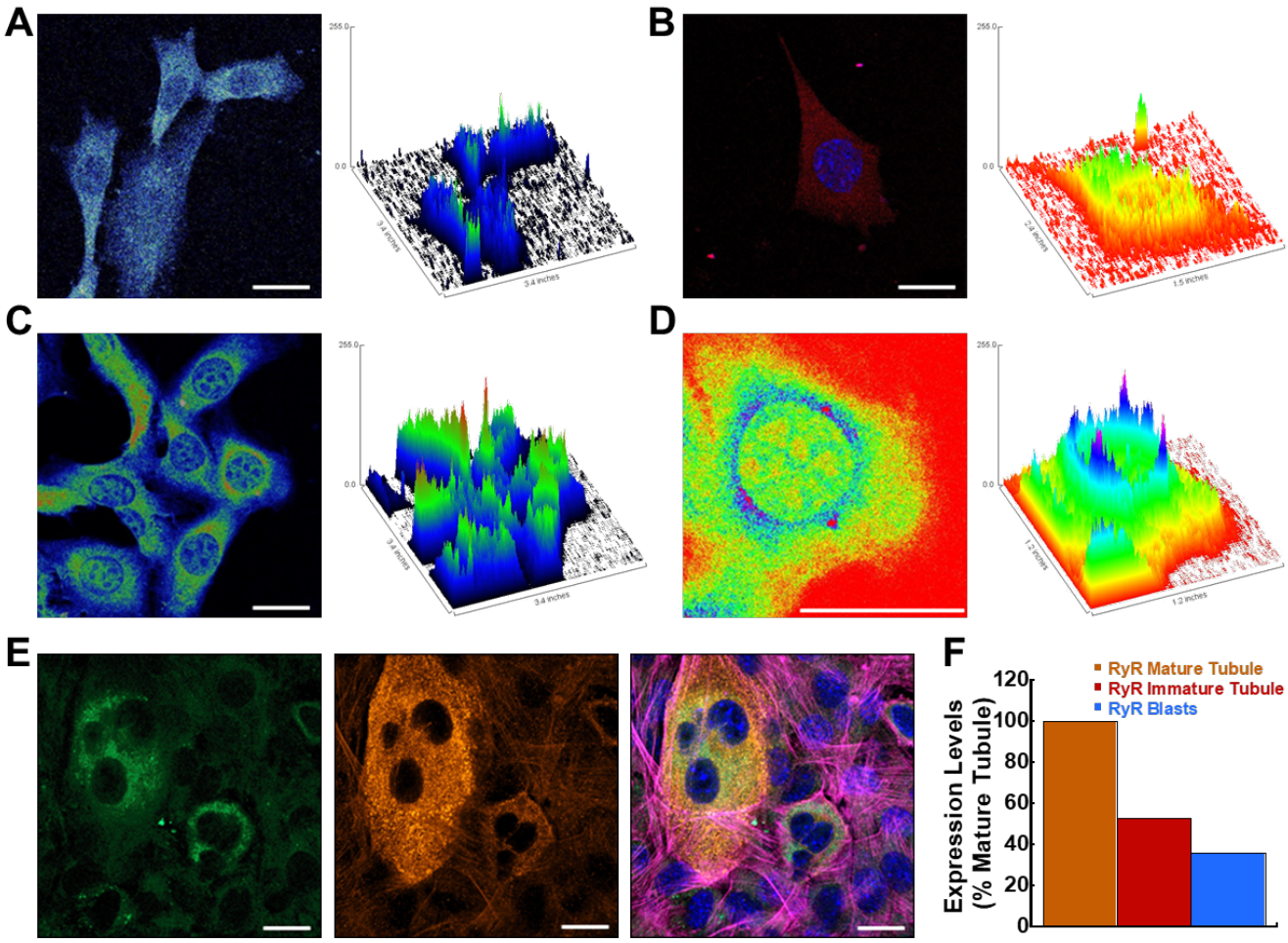

Supplemental Figure 5. Differential cellular distribution of RyR and SERCA in C2C12 cells, related to Figure 4 and Figure 5.

A&C. Confocal image of RyR **(A)** or SERCA1/SERCA2 **(C)** under rainbow RGB colors where red is high signal and blue is the low signal. *Right,* surface plot of these cells. **B&D.** A single C2C12 cell under spectrum colors where purple is the high signal and red is the low signal for RyR **(B)** or SERCA1/SERCA2 **(D)**. *Right,* surface plot of the cell. **E.** G-CatchER^{+} (green), RyR (orange), Phalloidin (magenta) and DAPI (blue) in C2C12 cells. **F.** RyR expression for blasts (single nuclei), immature tubule (2-3 indistinct nuclei), and mature tubule (≥ 3 distinct nuclei). 1.9 fold more RyR is found in mature tubule over forming tubule and 2.8 fold more in tubule versus blast cells. Scale bars are 20 μm.

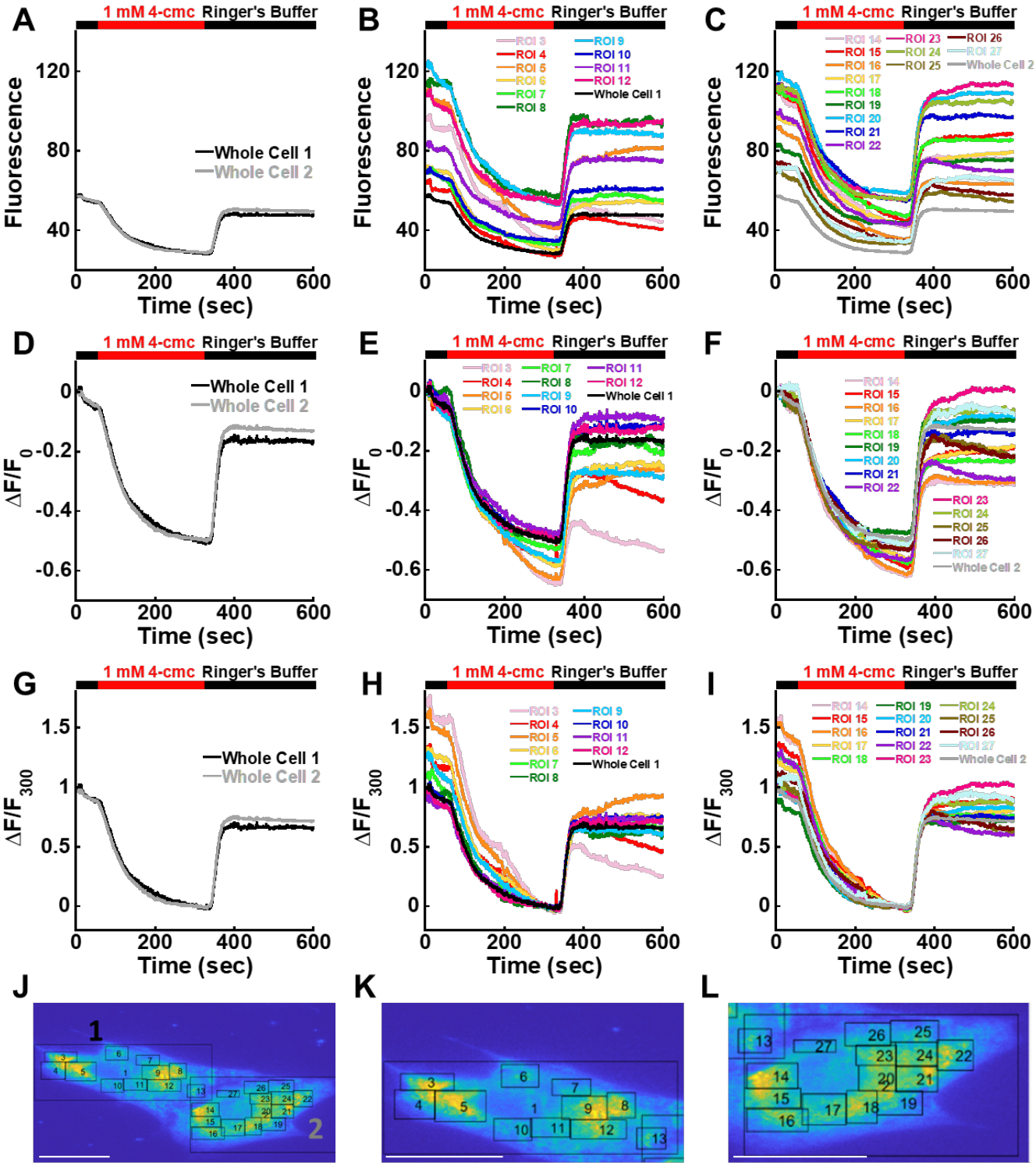

Supplemental Figure 6. G-CatchER⁺ monitors regional differential responses, related to Figure 4.

A-I. C2C12 cells transfected with G-CatchER⁺ and treated with 1 mM 4-cmc. The cells were examined as raw unprocessed data (**A-C**), normalized to starting as $(F\text{-}F_0)/F_0$ (**D-F**), and normalized to release as $(F\text{-}F_{300})/F_{300}$ (**G-I**). There is a large variance in response between the ROIs compared to the whole cell analysis, especially on the recovery phase. **J.** The whole cells where cell 1 is black and cell 2 is gray for plots A, D, and G. K. ROIs by number 3-12 on cell 1 from J as plotted in B, E, and H. L. ROIs by number 14-27 on cell 2 from J as plotted in C, F, and I. Scale bars are 20 μm.

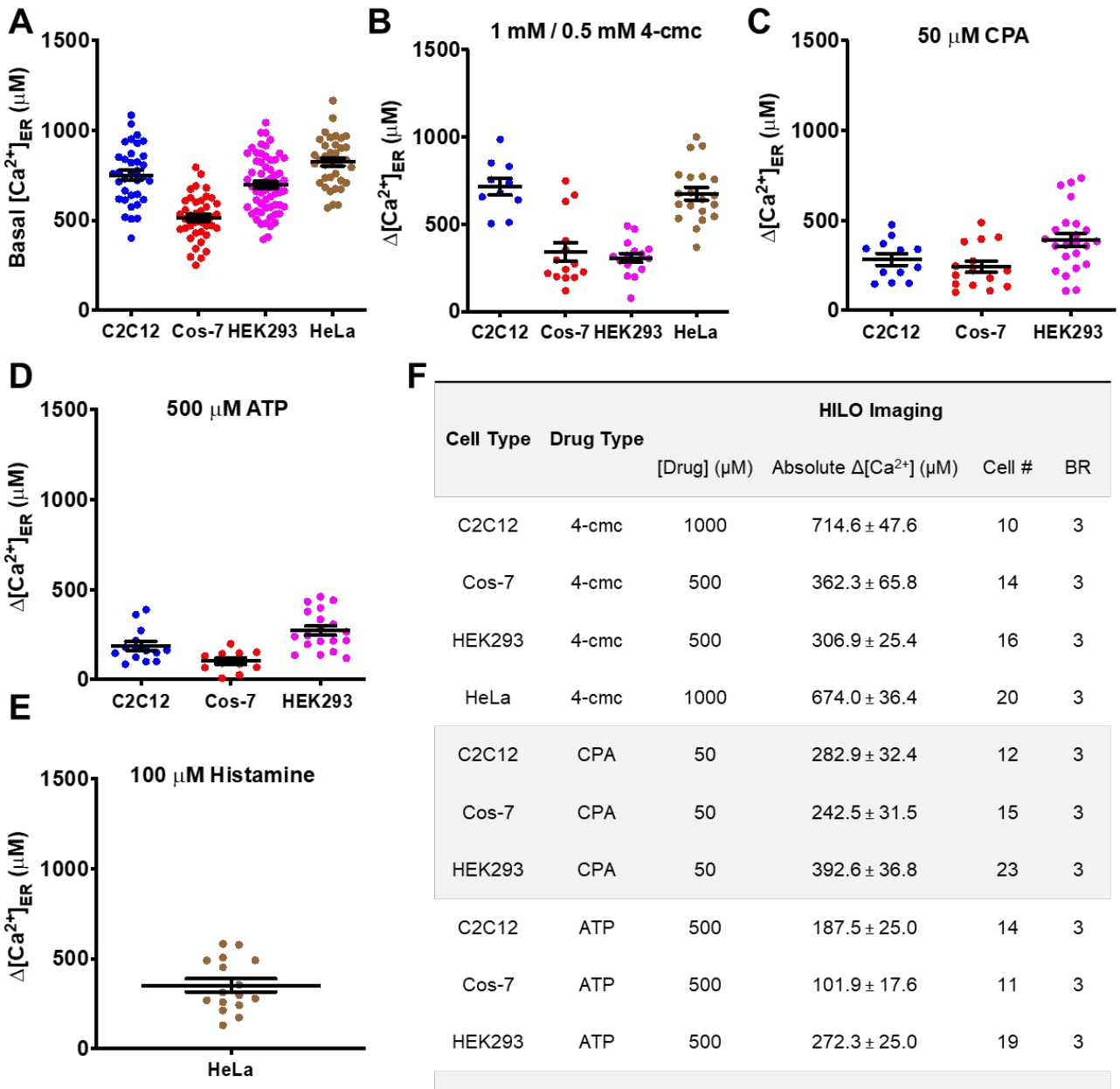

F

Cell Type	Drug Type	HILO Imaging			
		[Drug] (μM)	Absolute Δ[Ca²⁺] (μM)	Cell #	BR
C2C12	4-cmc	1000	714.6 ± 47.6	10	3
Cos-7	4-cmc	500	362.3 ± 65.8	14	3
HEK293	4-cmc	500	306.9 ± 25.4	16	3
HeLa	4-cmc	1000	674.0 ± 36.4	20	3
C2C12	CPA	50	282.9 ± 32.4	12	3
Cos-7	CPA	50	242.5 ± 31.5	15	3
HEK293	CPA	50	392.6 ± 36.8	23	3
C2C12	ATP	500	187.5 ± 25.0	14	3
Cos-7	ATP	500	101.9 ± 17.6	11	3
HEK293	ATP	500	272.3 ± 25.0	19	3
HeLa	Histamine	100	351.6 ± 36.3	16	3

Supplemental Figure 7. Quantitative measurement of G-CatchER⁺ in different cell lines following addition of stimulatory or inhibitory agents, related to Table 1.

A. Basal ER Ca^{2+} estimation using G-CatchER⁺ in different cell lines. **B-F.** Estimated absolute ER Ca^{2+} change in response to 4-cmc, CPA, ATP and histamine in different cell lines using G-CatchER⁺.

Supplementary Table 1. Determined and reported Kd values for G-CatchER$^+$ and other sensors, related to Figure 1.

Sensor Variant	λ_{ex} (nm)	0 mM KCl Buffer		KCl Buffer		Other Buffer	
		K_d (mM)	F_{max}/F_{min}	K_d (mM)	F_{max}/F_{min}	K_d (mM)	F_{max}/F_{min}
CatchER	488	0.2 ± 0.1	1.6 ± 0.1	0.9 ± 0.2	1.1 ± 0.2	-----	-----
G-CatchER-X	488	0.3 ± 0.1	2.1 ± 0.1	1.7 ± 0.1	1.3 ± 0.1	-----	-----
G-CatchER-XY	488	2.0 ± 0.6	1.5 ± 0.1	0.8 ± 0.1	1.2 ± 0.1	-----	-----
G-CatchER-XZ	488	1.0 ± 0.2	1.5 ± 0.1	5.1 ± 1.2	1.1 ± 0.1	-----	-----
G-CatchER$^+$	488	1.2 ± 0.2	1.6 ± 0.1	-----	-----	-----	-----
D1ER	436 (CFP)	-----	-----	-----	-----	0.08	-----
	500 (YFP)	-----	-----	-----	-----	60	-----
G-CEPIA1er	499 (-Ca^{2+})	-----	-----	0.67 ± 0.02	4.7 ± 0.3	-----	-----
GCamP6-150	485	-----	-----	0.15	45.0	-----	-----

Zero KCl and KCl buffers are 10 mM Tris pH 7.4 with or without 150 mM KCl. Data represents mean ± SD. Kd – dissociation constant, λex – excitation wavelength, Fmax/Fmin – dynamic range in response to Ca2+ calculated using the fluorescence at maximal saturation divided by the fluorescence with no Ca2+ present. Data collected at room temperature. Samples prepared in 10 mM Tris pH 7.4 with or without 150 mM KCl. Fluorescence slit widths were 0.25 mm for excitation and emission. Dashed lines indicate data not available. G-CatchER-X is S175G mutation, G-CatchER-XY is S175G and Y39N mutation, G-CatchER-XZ is S175G and S30R mutation, and G-CatchER+ is S175G, Y39N and S30R mutations. All CatchER variants were done in 0 mM KCl buffer and 150 mM KCl buffer. GCamP6-150 was done in 100 mM KCl and 50 mM MOPS buffer. G-CEPIA1er was done in KCl MOPS buffer. D1ER done in undisclosed buffer8,35.

Supplementary Table 2. Ca^{2+} effect on the optical properties of G-CatchER^{+} and other CatchER variants *in vitro*, related to Figure 1.

Variant	[a]ϕ		[b]Ɛ ($mM^{-1}cm^{-1}$)		[c]Brightness ($mM^{-1}cm^{-1}$)	
	0 mM Ca^{2+}	5 mM Ca^{2+}	0 mM Ca^{2+}	5 mM Ca^{2+}	0 mM Ca^{2+}	5 mM Ca^{2+}
CatchER	0.78 ± 0.01	0.57 ± 0.01	7.50 ± 0.01	14.88 ± 0.15	5.47 ± 0.03	8.48 ± 0.01
G-CatchER-X	0.80 ± 0.01	0.83 ± 0.03	11.00 ± 0.05	14.14 ± 0.01	8.74 ± 0.13	11.81 ± 0.36
G-CatchER^{+}	0.70 ± 0.01	0.64 ± 0.01	10.52 ± 0.16	15.15 ± 0.04	7.27 ± 0.18	9.72 ± 0.05
149E	0.59 ± 0.01	0.51 ± 0.01	25.40 ± 0.06	40.00 ± 0.09	14.91 ± 0.07	20.40 ± 0.10
149E Y39N	0.59 ± 0.01	0.52 ± 0.01	22.68 ± 0.07	37.30 ± 0.12	13.34 ± 0.12	19.46 ± 0.18
149E S30R	0.68 ± 0.01	0.58 ± 0.01	17.61 ± 0.16	34.66 ± 0.09	11.96 ± 0.12	20.28 ± 0.11

Data presented is mean ± SD. Samples prepared in 10 mM Tris pH 7.4 with 10 µM EGTA. Experiments conducted at room temperature. Fluorescence excited at 488 nm and fluorescence excitation and emission slit widths were 0.1 mm and 0.6 mm, respectively. EGFP quantum yield was measured as 0.6 and used as the reference in the calculation. The 44 $mM^{-1}cm^{-1}$ extinction coefficient at 447 nm absorbance peak for all FPs was used to calculate the extinction coefficient of the variants.

[a]ϕ quantum yield is the ratio of photons emitted to photons absorbed.

[b]Ɛ extinction coefficient is how strongly a compound absorbs light at a given wavelength.

[c]Brightness is the perceived intensity of color. ϕ x Ɛ

Supplementary Table 3. Chromophore pK_a of G-CatchER$^+$ and other CatchER variants, related to Figure 1.

Variant	[a]pK_a	
	0 mM Ca^{2+}	5 mM Ca^{2+}
[b]CatchER	7.59 ± 0.03	6.91 ± 0.03
G-CatchER-X	7.71 ± 0.01	6.78 ± 0.00
G-CatchER$^+$	7.37 ± 0.01	6.80 ± 0.01
149E	6.47 ± 0.02	6.44 ± 0.01

Data presented is mean ± SD from fluorescence intensities were excited at 488 nm. Experiment done at room temperature. pH values were recorded before and after data collection. Final values were used for curve fitting.
[a]pK_a is the negative log of the acid dissociation constant which reflects the protonation state of the variant chromophore.
[b]Reported values of CatchER are from the cited reference.

Transparent Methods

Chemicals and Reagents

The *E. coli.* strain DH5α, the plasmid vector pCDNA3.1(+), was purchased from Invitrogen. All the restriction enzymes, T4 DNA ligase, and T4 polynucleotide kinase (PNK) were purchased from New England Biolabs. DNA sequencing for all clones was carried out by GENEWIZ Inc. Plasmid extraction was carried out using the QIAGEN mini-prep and maxi-prep kits. C2C12, Cos-7, HEK-293 and HeLa cells were purchased from American Type Culture Collection (ATCC). (S)-3,5-DHPG (10 mM stock in buffer) and thapsigargin (1 mM stock in DMSO) were from Tocris. 4-cmc (100 mM stock in buffer), CPA (50 mM stock in DMSO), histamine (100 mM stock in buffer) and ATP (100 mM stock in buffer) were from Sigma-Aldrich. ER-Tracker Red, Alexa Fluor™ 633 Phalloidin and ProLong gold antifade mountant with DAPI were from Invitrogen. Mouse anti-ryanodine receptor antibody [34C], rabbit anti-ryanodine receptor antibody [EPR21796], mouse anti-SERCA1 ATPase antibody [VE121G9] and mouse anti-SERCA2 ATPase antibody [2A7-A1] were from abcam. pCMV-G-CEPIA1er was a gift from Dr. Yubin Zhou at Texas A&M University.

Cloning of G-CatchER$^+$

CatchER was designed as previously detailed(Tang et al., 2011). To create G-CatchER$^+$ containing the S175G, S30R, and Y39N mutations, point mutations were incorporated sequentially into CatchER in both vectors using 5'-AAGTTCAGCGTGCGCGGCGAGGGCGAG-3' and 5'-CTCGCCCTCGGCGCGCACGCTGAACTT-3' for S30R, 5'-GGCGATGCCACCAACGGCAAGCTG-3' and 5'-CAGCTTGCCGTTGGTGGCATCGCC-3' for Y39N, and 5'-GAGGACGGCGGCGTGCAGCT-3' and 5'-AGCTGCACGCCGCCGTCCTC-3' for S175G. G-CatchER$^+$ was cloned into the pcDNA3.1+ vector using BamH1 and EcoR1 restriction enzyme sites. pDsRed2-JP45 was kindly provided by Dr. Francesco Zorzato. To create the G-CatchER$^+$-JP45 fusion construct, dsRed was replaced with CatchER using BamH1 and Not1 restriction sites. Proper insertion of CatchER at the C-terminus of JP45 was confirmed by DNA sequencing using the forward primer 5'-GAGAAGCCAAGTAAAGGGGAGAAACTGAAG-

3’ representing a small sequence of DNA at the C-terminus of JP45. The S175G, S30R, and Y39N mutations were then added to the CatchER-JP45 construct to make G-CatchER^{+}-JP45.

Expression and purification of G-CatchER^{+} and variants

The GECI CatchER was created to monitor Ca^{2+} transients in the ER/SR and measure Ca^{2+} concentration in said organelles through a novel mechanism where the binding of Ca^{2+} on the surface of the protein induces an increase in fluorescence intensity. Because of improper formation of chromophore of CatchER at 37°C in mammalian cells (Tang et al., 2011), the probe was optimized to improve the fluorescence at 37°C resulting in the G-CatchER^{+} series of variants. To obtain large amounts of the probes for *in vitro* analysis, the sensors were expressed and purified with high yield as previously detailed (Zhang et al., 2013). Briefly, pET28a vectors containing variant DNA were transformed into BL21(DE3) gold cells. Variants were expressed at 25°C following the addition of 0.2 mM IPTG in Luria Bertani (LB) media with 30 mg/mL of kanamycin. After centrifugation, cell pellets were re-suspended in 20-30 mL of lysis buffer (20 mM Tris, 100 mM NaCl, 0.1% Triton X-100, pH 8.0) and sonicated. The resulting lysate containing the protein of interest was centrifuged, and the supernatant was filtered and applied to a 5 mL Ni^{2+}-NTA HiTrap^{TM} HP chelating column (GE Healthcare) for HisTag purification using an imidazole gradient. To ensure protein purity and complete removal of imidazole, pure protein fractions were concentrated to 1 mL and buffer exchanged on a Superdex 200 gel filtration column (GE Healthcare) using 10 mM Tris pH 7.4 at 1 mL/min. Samples were taken during the expression and purification processes for SDS-PAGE analysis.

To determine if the mutations did improve the thermostability and brightness of the sensor at 37°C, each variant, including CatchER, was expressed in C2C12 myoblast cells at 37°C and imaged using a Leica DM6000 fluorescence microscope using previously established protocols (Reddish et al., 2017). C2C12 cells were seeded at a density of 40% and transfected on 22 mm x 40 mm glass microscope slides (Fisherbrand®) in 6 cm dishes. Images were taken from 8 fields of view on each slide. The intensity of the cells from each area was quantified using Image J and plotted with error using K-graph.

in vitro K_d of G-CatchER$^+$ and variants using fluorescence spectroscopy

Fluorescence measurements of G-CatchER$^+$ with increasing Ca^{2+} concentrations were done in order to obtain the affinity of the sensor for Ca^{2+} *in vitro*. Samples of 10 µM sensor with 5 µM ethylene glycol tetra acetic acid (EGTA) were prepared in triplicate in 1 mL volumes in 10 mM Tris, pH 7.4. The samples were placed in quartz fluorescence cuvettes, and metal ion was titrated into each sample, in a step wise manner, using 0.1 M and 1 M metal stock solutions. The fluorescence response of the sensor to increasing Ca^{2+} concentrations was monitored using a fluorescence spectrophotometer (Photon Technology International, Canada) with the *Felix32* fluorescence analysis software. Slit widths were set at 0.25 or 0.3 mm for excitation and emission. The samples were excited at 395 nm and 488 nm with emission collected from 410-600 nm for 395 nm excitation and from 500-600 nm for 488 nm excitation. The absorbance spectra before and after titration were obtained using a Shimadzu UV-1601 spectrophotometer. Fluorescence and absorbance traces were plotted using Kalidegraph (KGraph). The data was normalized to show the relative change in relation to the basal fluorescence using the following equation,

$$y = \frac{(F - F_{min})}{(F_{max} - F_{min})} \qquad \text{equation 1}$$

where F is the fluorescence intensity at any point, F_{min} is minimum fluorescence intensity, and F_{max} is the maximum fluorescence intensity. The normalized data was then plotted and fitted in KGraph to obtain the dissociation constant (K_d) using the following equation for 1:1 binding,

$$\frac{[PM]}{[P_T]} = \frac{[M_T]}{K_d + [M_T]} \qquad \text{equation 2}$$

where [PM] is the concentration of protein-metal complex, $[P_T]$ is the total protein concentration, $[M_T]$ is the total metal concentration, and K_d is the dissociation constant. $[PM]/[P_T]$ represents the change in complex formation. A complete derivation of the 1:1 binding equation was done in previous work(Zhang et al., 2013). To determine the Ca^{2+} K_d at physiological concentrations of salt, Tris buffer and KCl were dissolved in H_2O to make the final concentrations of each 10 mM and 150 mM, respectively, and the pH was adjusted to 7.4. Subsequent titrations proceeded as previously stated.

Stop flow kinetics for G-CatchER$^+$

The kinetics of G-CatchER$^+$ and G-CEPIA1er were determined using a SF-61 stopped flow spectrofluorometer (10-mm path length, 2.2 ms dead time at room temperature; Hi-Tech Scientific) at room temperature. For G-CatchER$^+$, fluorescence intensity changes were recorded with a 510/30 nm band pass filter with excitation at 488 nm; whereas, for G-CEPIA1er, a 530 nm long pass filter with excitation at 498 nm was used. For association kinetics, G-CatchER+ and G-CEPIA1er in 0 Ca^{2+} buffer were mixed with the same buffer containing increasing concentration of Ca^{2+}. For disassociation kinetics, G-CatchER$^+$ and G-CEPIA1er were examined in a buffer with concentration of Ca^{2+} around K_d and were mixed with 5 mM EGTA. The raw data was fitted using either monoexponential (equation 3) or biexponential (equation 4) equations.

$$F = A1 \times \exp(R1 \times t) + C \qquad \text{equation 3}$$

$$F = A1 \times \exp(-R1 \times t) + A2 \times \exp(-R2 \times t) + C \qquad \text{equation 4}$$

A1 and A2, the amplitude of the fluorescence change at the first phase and second phase; R1 and R2, the observed rate constant at the first phase and second phase; and t, the time.

Fluorescence lifetime measurements

G-CatchER$^+$ in H_2O was exchanged by D_2O (95% D) and the final pH and pD were adjusted to 7.4 and 7.8, respectively. For neutral and anionic forms of G-CatchER$^+$, a 372 nm laser was used to excite G-CatchER$^+$ and emission at 440 nm and 510 nm were detected, accordingly. 1024 data points were collected for the neutral form of G-CatchER$^+$ in 5 ns, however, for the anionic form, 1024 data points were collected in 20 ns. All measurements were carried out at 25ºC. The time course of fluorescence decay was deconvoluted by the program FFIT developed and fitted using an exponential equation (Bayley et al., 1984).

Cell culture and transfection of G-CatchER$^+$ and G-CatchER$^+$-JP45

Cell culture and transfection of G-CatchER$^+$ and G-CatchER$^+$-JP45 was done and modified based on established protocols (Reddish et al., 2017). We chose HEK293 and Cos-7 cells for their high transfection ability, their accessibility, and their rapid growth. Cos-7 cells have a greater cytosol to nuclear ratio and are also very flat which, improves focusing during image acquisition. C2C12 myoblast cells were chosen because they are non-differentiated skeletal muscle cells that can differentiate into myotubes which could be used to compare differences in calcium transients between immature and maturing cells. These cells were maintained in Corning™ Dulbecco's modified Eagle's medium (DMEM) with L-Glutamine, 4.5g/L supplemented with 10% fetal bovine serum (FBS) and high glucose (4.5 g/L) at 37°C. G-CatchER$^+$ was transfected into cells using Lipofectamine 3000 (Life Technologies) by following the manufacturer's instructions. HEK293, Cos-7 or HeLa cells were seeded onto sterilized 22 mm x 40 mm glass microscope slides in 6 cm dishes. The next day, cells were transfected with G-CatchER$^+$ or G-CatchER$^+$-JP45 cDNA and incubated for 4-6 h at 37°C. After incubation, cells were washed with 5-6 mL of HBSS and replaced with 3 mL of fresh DMEM and incubated for 48 h at 37°C to allow expression of G-CatchER$^+$ and G-CatchER$^+$-JP45. For C2C12 myoblast cells, transfection material was incubated for 24 h at 37°C and then removed and imaged as stated above. For myotube imaging and staining, slides were pretreated with laminin to allow high confluency cell growth. The first transfection for myotubules was done as stated above for C2C12 cells using G-CatchER$^+$ or G-CatchER$^+$-JP45 on day 0, then on day 2 the transfection was repeated, and again on day 4 the transfection was repeated where imaging was done on days 6-8. Washing with fresh DMEM was done after each transfection.

Primary hippocampal neuron cultures were generated from postnatal day 0-1 mice as previously described (Wall et al., 2018). Neurons were maintained in neuronal feeding media (Neurobasal media, ThermoFisher Scientific) containing 1% GlutaMAX (ThermoFisher Scientific), 2% B-27 (ThermoFisher Scientific), 4.8 µg/mL 5-Fluoro-2'-deoxyuridine (Sigma), and 0.0002 mg/mL Gentamicin (Sigma) and fed every 3-4 days via half neuronal feeding media exchange. At 11-12 days *in vitro* cells were transfected with G-CatchER$^+$ DNA and mCherry (used as a cell fill) DNA using Lipofectamine 2000 Reagent (ThermoFisher Scientific) using a modified protocol (Mabb et al., 2014).

The electroporation procedure was as described previously (DiFranco et al., 2009). Briefly, 8- to 14-week-old mice were anaesthetized using isofluorane, and 7.5 µl of 2 mg/ml Hyaluronidase in RNase-free Tyroide's Buffer (Sigma-Aldrich, #H3506) was injected under the footpad. The mice were left 1 h under supervision, and subsequently, the pcDNA^{+}3.1 plasmids carrying G-CatchER^{+} and G-CatchER^{+}-JP45 were injected into the footpad. Ten minutes post-injection, FDBs were electroporated using acupuncture needles placed parallel and perpendicular to the long axis of the foot (with 1 cm distance), and twenty pulses (100v/cm, 20 ms duration and 1 Hz of frequency) were given. Six to ten days post–transfection, the mice were sacrificed and FDBs were isolated by enzymatic dissociation at 37°C for 60 min in Krebs Ringer solution without Ca^{2+} (pH 7.4), containing 0.2% collagenase I (Sigma-Aldrich, C-0130). Enzymatic digestion was terminated by washing the muscle with Tyrode's solution (pH 7.4) and single fibers were isolated.

Confocal imaging of G-CatchER^{+} and G-CatchER^{+}-JP45

We used confocal laser scanning microscopy (CLSM) Zeiss LSM800 on fixed cells. These cells were stained with either BODIPY ER-Tracker Red (Invitrogen) per their protocol at 1 µM for staining the ER, Alexa Fluor™ 633 Phalloidin (Invitrogen) per their protocol for staining actin, anti-ryanodine receptor antibody [34C] (abcam), anti-ryanodine receptor antibody [EPR21796] (abcam), anti-SERCA1 ATPase antibody [VE121G9] (abcam), anti-SERCA2 ATPase antibody [2A7-A1] (abcam), and all with ProLong gold antifade mountant with DAPI (Invitrogen) for staining the nucleus. G-CatchER^{+} or G-CatchER^{+}-JP45 were transfected into the cells two days before fixing for blast cells and were triple transfected over one week for myotubules. Cells were fixed with 3.7% Thermo Scientific™ Pierce™ 16% Formaldehyde (w/v), Methanol-free, permeabilized with 0.1% Triton X-100, and non-specific binding was blocked with 1-5% Bovine Serum Albumin (BSA) all in phosphate buffered saline (PBS).

As for confocal imaging of G-CatchER^{+} or G-CatchER^{+}-JP45 in C2C12 myoblasts and myotubes, G-CatchER^{+} or G-CatchER^{+}-JP45 were transfected into the cells two days before fixation. The distribution of G-CatchER^{+} is more widespread than G-CatchER^{+}-JP45 which is more concentrated near certain sections of the cell than other,

presumably the longitudinal SR. Both sensors overlay well with ER-Tracker Red, showing that although their specific ER locations may differ they still are both situated solely in the ER. HILO microscopy more thoroughly shows the network type pattern of the ER in the cells expressing G-CatchER$^+$.

Epifluorescence imaging of G-CatchER$^+$

G-CatchER$^+$ was transiently transfected into cells grown on coverslips and cultured for 48 h at 37°C. Cells were washed twice with 2 mL of physiological Ringer buffer (10 mM HEPES, 121 mM NaCl, 2.4 mM K_2HPO_4, 0.4 mM KH_2PO_4, 1.2 mM $MgCl_2$, 1.8 mM $CaCl_2$ at pH 7.4). The coverslips are mounted on a bath chamber and placed on the stage of a fluorescence microscope. The cells were illuminated with 488 nm and the fluorescence at an emission wavelength 510 nm was recorded in real time as the concentration of ER/SR Ca^{2+} was perturbed with 4-cmc, CPA, or ATP. All experiments were performed at room temperature on a Leica DM6100B inverted microscope with a Hamamatsu cooled EM-CCD camera and illuminated with a Till Polychrome V Xenon lamp.

HILO imaging of G-CatchER$^+$ and G-CatchER$^+$-JP45

HILO microscopy was accomplished using a Nikon TiE inverted microscope with Andor Ixon Ultra 888 EMCCD Camera. Briefly, a fiber coupled 488 nm laser (Oxxius) was collimated and introduced into the optical train of the microscope. The laser was then focused at the back focal plane of a 100X TIRF objective (N.A. 1.49, Nikon) by using an achromatic optical lens (Thorlabs) with 200 mm focal length. The laser collimation system and focusing lens were both mounted on a mechanic translation stage (Thorlabs) so that its optical axis of incident laser could be laterally shifted to change the incident angle of laser at the cell-coverslip interface. The HILO imaging condition was achieved by operating at sub-critical angles of the total internal reflection. Since the thickness of cells as well as the depth of ER structure varies among individual cells, the best HILO imaging conditions were achieved by carefully tuning the incident angle of the excitation laser. Moreover, the epifluorescence images used for comparing with HILO imaging was taken by setting the incident angle at 0 degrees. Large scale data

analysis of live cell imaging of G-CatchER$^+$ and G-CatchER$^+$-JP45 using HILO imaging was done with self-written MATLAB script.

Correlation between G-CatchER$^+$ and ER proteins

C2C12 cells were cultured in Ibidi flow chamber µ-Slide I Luer 0.8 mm and transfected using Lipofectamine 3000 at 2 µg/mL of G-CatchER$^+$ DNA. Imaging of the flow chamber was done using HILO imaging microscope as described above. In live cell experiments, the 4-cmc drug was introduced into the flow chamber by using a syringe pump at a flow rate of 1 mL/min. Then we mark the area on the outside of the chamber using marker and draw next to the imaged cell on bright field. The cells were immediately fixed after live cell imaging experiments with 3.7% Thermo Scientific™ Pierce™ 16% formaldehyde (w/v), methanol-free in PBS for 15 mins at room temperature. Cells were washed with 0.1% Triton X-100 in PBS, and non-specific binding was blocked with 5% BSA in PBS for 1 hour. The samples were incubated in 1% BSA with 1:500 of anti-GFP antibody (abcam), 1:100 of anti-ryanodine receptor antibody [EPR21796] (abcam), and 1:250 of both anti-SERCA1 ATPase antibody [VE121G9] (abcam) and anti-SERCA2 ATPase antibody [2A7-A1] (abcam) overnight at 4°C. Cells were aspirated and washed three times with PBS at room temperature then incubated at 1:500 with goat anti-chicken Alexa Fluor 488 (abcam) and 1:250 with both goat anti-mouse Alexa Fluor 555 (abcam) and goat anti-rabbit Alexa Fluor 633 (Thermofisher). After rinsing 3 times (10 min each time) in PBS the slides were mounted with Invitrogen™ ProLong™ Gold Antifade Mountant with DAPI for staining the nucleus. We used confocal laser scanning microscopy (CLSM) Zeiss LSM800 on fixed cells and Airyscan technology. Correlation analysis between G-CatchER$^+$ signal and ER proteins (RyR, SERCA) was analyzed using self-written MATLAB script.

Neuron imaging

For live imaging of G-CatchER$^+$ in neuron cultures, G-CatchER$^+$-transfected neurons were transferred to artificial cerebrospinal fluid (ACSF; 124 mM NaCl, 3 mM KCl, 2 mM $CaCl_2$, 2 mM $MgCl_2$, 10 mM HEPES, 10 mM D-Glucose, pH 7.4) pre-warmed to 37°C. Neurons were imaged using HILO microscopy at 2 frames per second

with the protocol and equipment discussed above. Once a G-CatchER$^+$ transfected neuron was identified, it was inspected using the mCherry cell fill for healthy cell morphology. G-CatchER$^+$ signal was acquired at baseline, whereupon a drug treatment was gently washed in (1 mM 4-cmc, 50 µM CPA, or 100 µM DHPG all in ACSF pre-warmed to 37°C) with a syringe connected to tubing that extended into the imaging chamber. Following imaging under treatment conditions, drugs were washed out with ACSF pre-warmed to 37°C. Maximum fluorescence (Fmax) of G-CatchER$^+$ was obtained by applying 50 µM ionomycin and 10 mM Ca^{2+}. Basal $[Ca^{2+}]_{ER}$ in different neuronal regions was calculated using an established method (de Juan-Sanz et al., 2017).

Drosophila strains and husbandry

All flies were maintained on standard cornmeal-molasses-agar media. All genetic crosses were raised at 29°C in 12:12 light:dark cycle. The following *Drosophila* stocks used in this study were obtained from the Bloomington *Drosophila* Stock Center: Mef2^{GAL4}: *y[1] w[*]; P{w[+mC]=GAL4-Mef2.R}3* (BDSC# 27390); UAS-GFP: *w[1118]; P{y[+t7.7] w[+mC]=10XUAS-IVS-mCD8::GFP}su(Hw)attP1* (BDSC# 32187); UAS-Sec61β::tdTomato: *w[1118]; P{y[+7.7] w[+mC]=20XUAS-tdTomato-Sec61beta}attP2* (BDSC# 64747), and the background genetic control strain: *w[1118]* (BDSC# 3605).

Molecular cloning and *Drosophila* transgenic production

We utilized Gateway cloning technology for generating the *UAS-G-CatchER*$^+$ plasmid. We performed cloning based on the Invitrogen protocol for MultiSite Gateway Pro Plus (Vector module (ref: 45-2100), BP Clonase (ref: 11789-020) and LR Clonase (ref: 12538-120)). We inserted G-CatchER$^+$ into the donor vector by performing a BP reaction with G-CatchER$^+$ in the pcDNA3.1 plasmid backbone and pDONR^{tm} 221 P5-P2. Next, we combined pENTR L1-20XUAS-R5 (Addgene# 32302) and pDONR^{tm} 221 P5-G-CatchER+-P2 (BP reaction product, this study) into the *Drosophila* destination vector pDESTsvaw (Addgene# 32318) by performing the LR reaction. *Drosophila* transgenic production was performed by GenetiVision Corporation (Houston, TX). PhiC31 integrase technology was used to insert *UAS-G-CatchER*$^+$ into the 2nd (VK1) and 3rd chromosome (VK20) *attP* landing sites.

in vivo imaging of genetically-encoded G-CatchER$^+$ in *Drosophila*

In vivo confocal imaging of muscle morphology and SR localization of G-CatchER$^+$ was performed as previously described (Turner et al., 2016, Patel and Cox, 2017). Briefly, we mount live, intact, 3rd instar *Drosophila* larvae on a microscope slide using 1:5 solution of diethyl ether and halocarbon oil. *Drosophila* larvae were imaged using a Zeiss LSM 780 laser scanning confocal microscope, where z-stacks imaged for muscle morphology were acquired using an Apochromat 20x lens and SR localization acquired using an Apochromat 40x objective lens.

Cold-evoked imaging of SR Ca^{2+} dynamics was performed as previously described (Turner et al., 2016, Patel and Cox, 2017). Intact, live, 3rd instar *Drosophila* larvae were mounted on microscope slide with water and coverslip, where the coverslip was secured by stage clips. A PE120 thermal stage and T95 system controller from Linkam Scientific Instruments were used for delivering temperature stimuli to *Drosophila* larvae. We used the following cold stimulation regimen: an initial 1 minute baseline recording at 25°C; ramp down to 10°C at a rate of 20°C/minute; hold at 10°C for 30 seconds; ramp up to 25°C at 20°C/minute to return to baseline, repeating this cold stimulus regimen two additional cycles for a total of three stimulations. G-CatchER$^+$ responses were recorded in intact, live *Drosophila* 3rd instar larvae using a Zeiss LSM 780 confocal with Neofluar 10x objective lens at 5.08 frames per second, 512 x 512 pixel resolution. G-CatchER$^+$ fluorescence was analyzed using Fiji (Schindelin et al., 2012) by creating a grid of 85 ROIs of 30 x 100 pixels. Percent $\Delta F/F_0$ for all animals and ROIs was calculated using a custom R script and the following equation: $^{\Delta F}/_{F_0} = \frac{F_{n\,frame} - average\ F_{frames\ 1-300}}{average\ F_{frames\ 1-300}}$

Drosophila larval locomotion assay

Larval locomotion assay was performed using 3rd instar *Drosophila* larvae. Larvae were placed on 2% agarose gel and allowed to acclimate for 5 minutes at 25°C. To obtain high signal to noise ratio, we illuminated the agarose gel and larvae from below and imaged larvae from above using a Nikon D5300 DSLR camera at 30 frames per second. We recorded larval locomotion for 5 minutes. Raw larval locomotion videos were uncompressed using video to video convertor (videotovideo.org). The background was removed from original videos and exported as an image sequence via custom Fiji scripts. Larval locomotion was tracked using FimTrack (Risse et al., 2017). Larval locomotion consists of peristaltic linear forward motion with saccadic turns

and reverse locomotion. Additionally, the larvae may collide with a barrier or other larvae, which impairs locomotion tracking. Therefore, we analyzed only continuous 1-minute long locomotion tracks, where individual larvae did not collide with one another. FimTrack data of individual videos was compiled and processed using custom R scripts (Wickham et al., 2019; Bengtsson, 2018; R Core Team, 2017; R Studio Team, 2020). tSNE analyses were performed in R using a publicly available library for tSNE (Krijthe, 2015).

Statistics

Error bars indicate mean ± SEM. Student's t tests or One-way ANOVA were used to determine the significant difference.

Supplemental References

BAYLEY, P., AHLSTROM, P., MARTIN, S. R. & FORSEN, S. 1984. The Kinetics of Calcium-Binding to Calmodulin - Quin-2 and Ans Stopped-Flow Fluorescence Studies. *Biochemical and Biophysical Research Communications,* 120**,** 185-191.

BENGTSSON, H. 2018. matrixStats: Functions that apply to rows and columns of matrices and to vectors. R package version 0.54.0. https://CRAN.R-project.org/package=matrixStats.

DE JUAN-SANZ, J., HOLT, G. T., SCHREITER, E. R., DE JUAN, F., KIM, D. S. & RYAN, T. A. 2017. Axonal Endoplasmic Reticulum Ca(2+) Content Controls Release Probability in CNS Nerve Terminals. *Neuron,* 93**,** 867-881 e6.

DIFRANCO, M., QUINONEZ, M., CAPOTE, J. & VERGARA, J. 2009. DNA transfection of mammalian skeletal muscles using in vivo electroporation. J Vis Exp.

KRIJTHE, J.H. 2015. Rtsne: T-distributed stochastic neighbor embedding using a Barnes-Hut implementation. URL: https://github.com/jkrijthe/Rtsne.

MABB, A. M., JE, H. S., WALL, M. J., ROBINSON, C. G., LARSEN, R. S., QIANG, Y., CORREA, S. A. & EHLERS, M. D. 2014. Triad3A regulates synaptic strength by ubiquitination of Arc. Neuron, 82, 1299-316.

PATEL, A. A. & COX, D. N. 2017. Behavioral and Functional Assays for Investigating Mechanisms of Noxious Cold Detection and Multimodal Sensory Processing in Drosophila Larvae. *Bio Protoc,* 7.

R CORE TEAM. 2017. R: A language and environment for statistical computing. R Foundation for Statistical Computing, Vienna, Austria. https://www.R-project.org.

R STUDIO TEAM. 2020. RStudio: Integrated development for R. RStudio, PBC, Boston, MA. http://www.rstudio.com

REDDISH, F. N., MILLER, C. L., GORKHALI, R. & YANG, J. J. 2017. Monitoring ER/SR Calcium Release with the Targeted Ca2+ Sensor CatchER+. *JoVE (Journal of Visualized Experiments)***,** e55822.

RISSE, B., BERH, D., OTTO, N., KLAMBT, C. & JIANG, X. 2017. FIMTrack: An open source tracking and locomotion analysis software for small animals. *PLoS Comput Biol,* 13**,** e1005530.

SCHINDELIN, J., ARGANDA-CARRERAS, I., FRISE, E., KAYNIG, V., LONGAIR, M., PIETZSCH, T., PREIBISCH, S., RUEDEN, C., SAALFELD, S., SCHMID, B., TINEVEZ, J. Y., WHITE, D. J., HARTENSTEIN, V., ELICEIRI, K., TOMANCAK, P. & CARDONA, A. 2012. Fiji: an open-source platform for biological-image analysis. *Nat Methods,* 9**,** 676-82.

TANG, S., WONG, H. C., WANG, Z. M., HUANG, Y., ZOU, J., ZHUO, Y., PENNATI, A., GADDA, G., DELBONO, O. & YANG, J. J. 2011. Design and application of a class of sensors to monitor Ca(2+) dynamics in high Ca(2+) concentration cellular compartments. *Proceedings of the National Academy of Sciences of the United States of America,* 108**,** 16265-16270.

TURNER, H. N., ARMENGOL, K., PATEL, A. A., HIMMEL, N. J., SULLIVAN, L., IYER, S. C., BHATTACHARYA, S., IYER, E. P. R., LANDRY, C., GALKO, M. J. & COX, D. N. 2016. The TRP Channels Pkd2, NompC, and Trpm Act in Cold-Sensing Neurons to Mediate Unique Aversive Behaviors to Noxious Cold in Drosophila. *Curr Biol,* 26**,** 3116-3128.

WALL, M. J., COLLINS, D. R., CHERY, S. L., ALLEN, Z. D., PASTUZYN, E. D., GEORGE, A. J., NIKOLOVA, V. D., MOY, S. S., PHILPOT, B. D., SHEPHERD, J. D., MULLER, J., EHLERS, M. D., MABB, A. M. & CORREA, S. A. L. 2018. The Temporal Dynamics of Arc Expression Regulate Cognitive Flexibility. *Neuron,* 98**,** 1124-1132 e7.

WICKHAM, H., FRANCOIS, R., HENRY, L. & MÜLLER, K. 2019. dplyr: A grammar of data manipulation. R package version 0.8.0.1. https://CRAN.R-project.org/package=dplyr.

ZHANG, Y., REDDISH, F., TANG, S., ZHUO, Y., WANG, Y. F., YANG, J. J. & WEBER, I. T. 2013. Structural basis for a hand-like site in the calcium sensor CatchER with fast kinetics. *Acta Crystallographica Section D-Biological Crystallography,* 69**,** 2309-2319.